universe

MDPI

Communication

Investigation of the Elliptic Flow Fluctuations of the Identified Particles Using the a Multi-Phase Transport Model

Niseem Magdy [1,*], Xu Sun [1], Zhenyu Ye [1], Olga Evdokimov [1] and Roy Lacey [2]

[1] Department of Physics, University of Illinois at Chicago, Chicago, IL 60607, USA; sunxuhit@gmail.com (X.S.); yezhenyu2003@gmail.com (Z.Y.); evdolga@uic.edu (O.E.)
[2] Department of Chemistry, State University of New York, Stony Brook, NY 11794, USA; roy.lacey@stonybrook.edu
* Correspondence: niseemm@gmail.com

Received: 16 August 2020; Accepted: 3 September 2020; Published: 6 September 2020

Abstract: A Multi-Phase Transport (AMPT) model is used to study the elliptic flow fluctuations of identified particles using participant and spectator event planes. The elliptic flow measured using the first order spectator event plane is expected to give the elliptic flow relative to the true reaction plane which suppresses the flow fluctuations. However, the elliptic flow measured using the second-order participant plane is expected to capture the elliptic flow fluctuations. Our study shows that the first order spectator event plane could be used to study the elliptic flow fluctuations of the identified particles in the AMPT model. The elliptic flow fluctuations magnitude shows weak particle species dependence and transverse momentum dependence. Such observation will have important implications for understanding the source of the elliptic flow fluctuations.

Keywords: collectivity; correlation; shear viscosity

1. Introduction

Many studies of the ultra-relativistic heavy-ion collisions at the Relativistic Heavy Ion Collider and the Large Hadron Collider show that an exotic state of matter named Quark-Gluon Plasma (QGP) is created in these collisions. A large number of studies are focused on identifying the dynamical evolution and the transport properties of the QGP.

In heavy-ion collisions, the produced particle azimuthal anisotropy measurements have been used in various studies to show the viscous hydrodynamic response of the QGP to the initial energy density spatial distribution produced in the early stages of the collisions [1–14]. The azimuthal anisotropy of the particles emitted relative to the reaction plane Ψ_R can be described by the Fourier expansion [15,16] of the final-state azimuthal angle ϕ distribution,

$$\frac{dN}{d\phi} \propto 1 + 2\sum_{n=1}^{\infty} v_n cos\left[n(\phi - \Psi_R)\right], \quad (1)$$

The first Fourier harmonic, v_1, is the directed flow; v_2 is called the elliptic flow, and v_3 is the triangular flow, etc. A wealth of information on the characteristics of the QGP has been gained via the anisotropic flow studies of directed and elliptic flow [17–19], higher-order flow harmonics $v_{n>2}$ [10,20–23], flow fluctuations [24–26] and different flow harmonics correlations [21,27–31].

Hydrodynamic studies suggest that anisotropic flow stems from the evolution of the medium in the presence of initial-state anisotropies, determined by the eccentricities ε_n. The v_2 and v_3 flow

harmonics are recognized to be linearly correlated to ε_2 and ε_3, respectively [7,28,32–38]. Therefore for these flow harmonics,

$$v_n = \kappa_n \varepsilon_n, \tag{2}$$

where κ_n encodes knowledge about the medium properties such as the specific shear viscosity (η/s) of the QGP. Accurate extraction of η/s requires certain restrictions on the initial-state models employed in such extractions. Such constraints can be achieved via measurements of the flow harmonics and the event-by-event flow fluctuations [39]. Flow fluctuations could be arising from several sources: one of which has attracted considerable attention is the initial eccentricity fluctuations [40–42]. Recent theoretical studies have begun to take into account initial conditions that include energy density fluctuations, initial flow [13,37,43], and the full shear stress tensor [44] at $\mu_B = 0$ and at $\mu_B > 0$ [45–48]. Also, the partonic structure inside the nucleons has been considered in Reference [49].

Recently, Reference [50] presented more realistic event-by-event fluctuating initial conditions, Initial Conserved Charges in Nuclear Geometry (ICCING), of not only the initial energy density profile but also the initial conserved charges of baryon number (B), strangeness (S), and electric charge (Q) density distributions. This work pointed out that while baryon number and electric charge have almost the same geometries to the energy density profile, the initial strangeness distribution is considerably more eccentric. Such an effect predicts that the elliptic flow fluctuations will be larger for the strange and multi-strange hadrons. This effect can be detected experimentally via studying the elliptic flow fluctuations of the identified hadrons.

The ratio between four-particles elliptic flow, $v_2\{4\}$, and the two-particles elliptic flow, $v_2\{2\}$, is often used to estimate the strength of the elliptic flow fluctuations as a fraction of the measured flow harmonic strength [51,52]. However, important caveats to studying the elliptic flow fluctuations using ($v_2\{4\}/v_2\{2\}$) for the identified hadrons are, first, the demand for high statistical power, and second, the multi-strange hadron identification process [53]. Consequently, the ratio of $v_2\{4\}/v_2\{2\}$ is of limited experimental use for carrying out these investigations for the multi-strange hadrons.

In this work, we investigate an alternative validation scheme, which employs the use of the first-order spectator event plane, Ψ_1^{SP}, along with the second-order event plane Ψ_2^{EP} to study the elliptic flow fluctuations of the identified hadrons. Here, the underlying notion is that v_2^{SP} (with respect to the spectator first-order event plane) will reduce the elliptic flow fluctuations due to the strong correlations between the Ψ_1^{SP} and the true reaction plane. Therefore, the ratio $v_2^{\mathrm{SP}}/v_2^{\mathrm{EP}}$ is expected to reflect the elliptic flow fluctuations.

For RHIC highest energy and using the STAR detector, we propose a similar investigation to be performed using the first-order spectator event plane from spectator neutrons, measured by the zero-degree calorimeters (ZDC) [54] and the second-order event plane using the new installed Event-Plane-Detector (EPD) [55]. Consequently, we think that conducting a similar experimental study will reveal important information about the elliptic flow fluctuations and will shed light on the ICCING scenario suggested in Reference [50].

2. Method

The current study is conducted with simulated events for Au+Au collisions at $\sqrt{s_{NN}}$ = 200 GeV, collected using the AMPT [56] model with the string-melting mechanism and hadronic cascade on. The AMPT model, which has been widely employed to study relativistic heavy-ion collisions [56–60,60–62], includes four main dynamical components: initial condition, parton cascade, hadronization, and hadronic rescatterings. The initial conditions take into account soft string excitations and the phase space distributions of minijet partons, which are produced by the Heavy-Ion Jet Interaction Generator model (HIJING) [63] in which the Glauber model with multiple nucleon scatterings are used to define the heavy-ion collisions initial state.

The partons scatterings are handled according to the Zhang's Parton Cascade (ZPC) model [64], which contain only two-body elastic scatterings with a cross-section defined as:

$$\frac{d\sigma}{dt} = \frac{9\pi\alpha_s^2}{2}(1+\frac{\mu^2}{s})\frac{1}{(t-\mu^2)^2}, \tag{3}$$

where $\alpha_s = 0.47$ is the strong coupling constant, μ is the screening mass and s and t are the Mandelstam variables. In the AMPT with the string-melting mechanism, the excited strings and minijet partons are melted into partons. The partons scatterings will lead to local energy density fluctuations, which are equivalent to the local transverse density of participant nucleons.

In the string-melting version and when partons stop interacting with each other, a quark coalescence model is used to couple partons into hadrons. Consequently, the partonic matter is then converted into hadronic matter and the hadronic interactions are given by the A Relativistic Transport (ART) model [65], which incorporates both elastic and inelastic scatterings for baryon–baryon, baryon–meson, and meson–meson interactions.

In this work, the centrality intervals are defined by selecting the impact parameter distribution, then the AMPT events are analyzed using (i) the event plane method and (ii) the multi-particle cumulant technique [66–69]. Using both methods, particle of interest (POI) comes from pseudorapidities $|\eta| < 1$, which matches the STAR experiment pseudorapidity acceptance, and with transverse momentum $0.1 < p_T < 4.0$ GeV/c.

The second-order event plane ($\Psi_2^{\rm EP}$), is estimated from the azimuthal distribution of final-state particles. The elliptic flow that will be obtained using this method will then be corrected with the corresponding event plane resolution (Res($\Psi_2^{\rm EP}$)) [16]. The $\Psi_2^{\rm EP}$ is reconstructed in a pseudorapidity range of $2.5 < |\eta| < 4.5$, which matches the STAR experiment EPD acceptance, and $0.1 < p_T < 2.0$ GeV/c:

$$\Psi_2^{\rm EP} = \frac{1}{2}\tan^{-1}\left[\frac{\sum\omega_i \sin(2\phi_i)}{\sum\omega_i \cos(2\phi_i)}\right], \tag{4}$$

where ϕ_i is the final-state azimuthal angle of particle i, and ω_i is its weight. The weight is chosen to be equal to p_T. Also, the first order spectator plane $\Psi_1^{\rm SP}$ is constructed using the AMPT spectator x and y position information. Using the spectator or the event planes we can give the elliptic flow as:

$$v_2^{\rm EP} = \frac{\langle\cos\left(2(\phi_i - \Psi_2^{\rm EP})\right)\rangle}{Res(\Psi_2^{\rm EP})}, \tag{5}$$

$$v_2^{\rm SP} = \frac{\langle\cos\left(2(\phi_i - \Psi_1^{\rm SP})\right)\rangle}{Res(\Psi_1^{\rm SP})}, \tag{6}$$

where Res($\Psi_2^{\rm EP}$) and Res($\Psi_1^{\rm SP}$) represent the resolution of the event planes. The event planes resolution is calculated using the two-subevent method [16].

On the other hand, the standard (subevents) cumulant methods framework is discussed in References [66–69]. In the standard cumulant method, the n-particle cumulants are constructed using particles from the $|\eta| < 1.0$ acceptance. Thus the constructed two- and four-particle correlations can be written as:

$$\langle v_n^2\rangle = \langle\langle\cos(n(\varphi_1 - \varphi_2))\rangle\rangle, \tag{7}$$

$$\langle v_n^4\rangle = \langle\langle\cos(n\varphi_1 + n\varphi_2 - n\varphi_3 - n\varphi_4)\rangle\rangle, \tag{8}$$

where, $\langle\langle\,\rangle\rangle$ represents the average over all particles in a single event, and then in average over all events, n is the harmonic number and φ_i expresses the azimuthal angle of the i^{th} particle. Then the four-particle elliptic flow harmonic can be given as:

$$v_2^4\{4\} \;=\; 2\,\langle v_2^2\rangle - \langle v_2^4\rangle. \tag{9}$$

In general, when the flow fluctuation σ is smaller than the true reaction plan elliptic flow $\langle v_2\rangle$ one can write [70,71]:

$$v_2^{\text{SP}} \;=\; \langle v_2\rangle \tag{10}$$

$$v_2^{\text{EP}} \;=\; \langle v_2\rangle + 0.5\frac{\sigma^2}{\langle v_2\rangle}. \tag{11}$$

Then the ratio $v_2^{\text{SP}}/v_2^{\text{EP}}$ can be used to estimate the strength of the elliptic flow fluctuations as a fraction of the measured flow harmonic (large value of $v_2^{\text{SP}}/v_2^{\text{EP}}$ indicates less fluctuations whereas a smaller value indicates large fluctuations),

$$\frac{v_2^{\text{SP}}}{v_2^{\text{EP}}} \;=\; \frac{\langle v_2\rangle}{\langle v_2\rangle + 0.5\frac{\sigma^2}{\langle v_2\rangle}} = \frac{1}{1+0.5\left(\frac{\sigma}{\langle v_2\rangle}\right)^2} \tag{12}$$

The reliability of this elliptic flow fluctuations extraction will depend on the strength of the correlations between the spectator plane and the reaction plane.

3. Results and Discussion

Panel (a) of Figure 1 compares the centrality dependence of the four-particle elliptic flow ($v_2\{4\}$) with the elliptic flow measured with respect to the event plane (v_2^{EP}) and spectators plane (v_2^{SP}). The comparison of the $v_2\{4\}$ and the v_2^{EP} shows larger v_2^{EP} magnitudes for $v_2\{4\}$. By contrast, the values for v_2^{SP} show good agreement with $v_2\{4\}$. Qualitatively, one expects such patterns due to the respective flow fluctuations contributions to $v_2\{4\}$ and v_2^{EP}. The experimental measurements for charge hadrons reported by the STAR experiment, shown in Figure 1b [18,72], also show good agreement between $v_2\{4\}$ and $v_2^{\text{SP}}(v_2^{\text{ZDC}})$, consistent with the AMPT simulations. Here, no attempt was made to improve the agreement between the model and the experimental results by varying the model parameters to influence the flow magnitude and its associated fluctuations [73–76]. We defer such an investigation to a future study. The ratio $v_2^{\text{SP}}/v_2^{\text{EP}}$, presented in panel (c) from AMPT, and data panel (d) serves as a metric for elliptic flow fluctuations. The $v_2^{\text{SP}}/v_2^{\text{EP}}$ decrease from central to peripheral collisions, consistent with the patterns expected when initial-state eccentricity fluctuations dominate. Note, however, that other sources of fluctuations could contribute.

The transverse momentum dependence of the $v_2\{4\}$, v_2^{EP} and v_2^{SP} are shown in Figure 2. This differential comparison further reflects the effect of the elliptic flow fluctuations on the v_2^{EP} which is highlighted in the ratio between v_2^{EP} and $v_2\{4\}$. Also a good agreement (within the errors) has been observed between the $v_2\{4\}$ and v_2^{SP}. The ratio $v_2^{\text{SP}}/v_2^{\text{EP}}$, presented in panel (b) presents the strength of the elliptic flow fluctuations which shows no p_T dependence, consistent with the preliminary STAR measurements [77].

The centrality dependence of the identified particles v_2^{EP} panel (a), v_2^{SP} panel (b) and v_2^{SP}/v_2^{EP} panel (c) are shown in Figure 3 for Au+Au collisions at $\sqrt{s_{NN}}$ = 200 GeV from the AMPT model. The results of v_2^{EP} and v_2^{SP} show the mass ordering effect on the observed magnitude. This mass ordering effect, which cancels out for the ratio v_2^{SP}/v_2^{EP}, presented in panel (c) indicates the domination of the initial-state eccentricity fluctuations in the AMPT model.

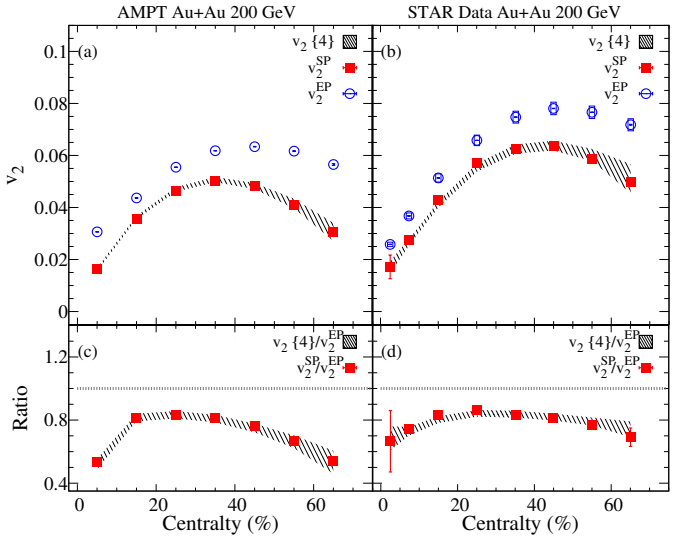

Figure 1. The charged particles centrality dependence of v_2^{SP} and v_2^{EP} are compared to the four-particles elliptic flow (hashed band) for Au+Au collisions at $\sqrt{s_{NN}}$ = 200 GeV from the A Multi-Phase Transport (AMPT) model panel (**a**). The charged particles centrality dependence of v_2^{SP} and v_2^{EP} are compared to $v_2\{4\}$ for Au+Au collisions at $\sqrt{s_{NN}}$ = 200 GeV from the STAR experiment [18,72] panel (**b**). The elliptic flow fluctuations represented by the ratios $v_2^{\mathrm{SP}}/v_2^{\mathrm{EP}}$ and $v_2\{4\}/v_2^{\mathrm{EP}}$ are presented in panels (**c**,**d**).

Figure 4 compares the p_T dependence of the identified particles v_2^{EP} panel (a), v_2^{SP} panel (b) and v_2^{SP}/v_2^{EP} panel (c) for $0-40\%$ Au+Au collisions at $\sqrt{s_{NN}}$ = 200 GeV from the AMPT model. The ratios v_2^{SP}/v_2^{EP} panel (c) (elliptic flow fluctuations) show week sensitivity to the p_T increase. The v_2^{EP} and v_2^{SP} vs. p_T show the expected mass ordering dependence, which cancels out for the ratio v_2^{SP}/v_2^{EP} vs. p_T, presented in panel (c), which further suggests that the elliptic flow fluctuations in the AMPT model are governed by initial-state fluctuations.

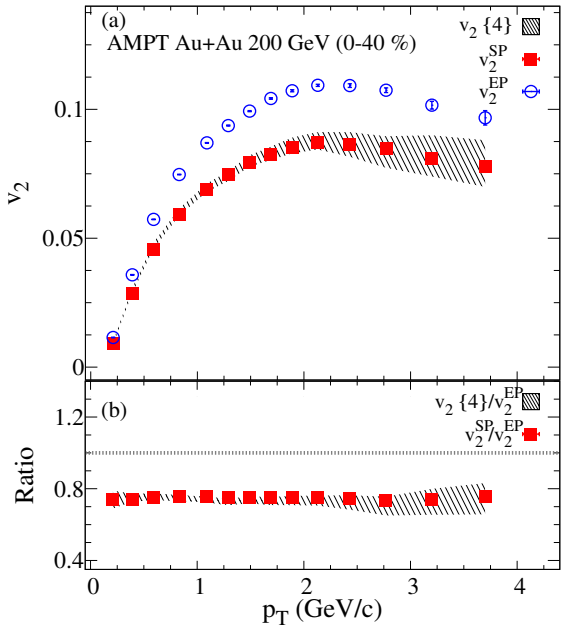

Figure 2. The charged particles p_T dependence of v_2^{SP} and v_2^{EP} are compared to the four-particles elliptic flow (hashed band) panel (**a**). The ratios $v_2^{\mathrm{SP}}/v_2^{\mathrm{EP}}$ and $v_2\{4\}/v_2^{\mathrm{EP}}$ are presented in panel (**b**) for Au+Au collisions at $\sqrt{s_{NN}}$ = 200 GeV from the AMPT model.

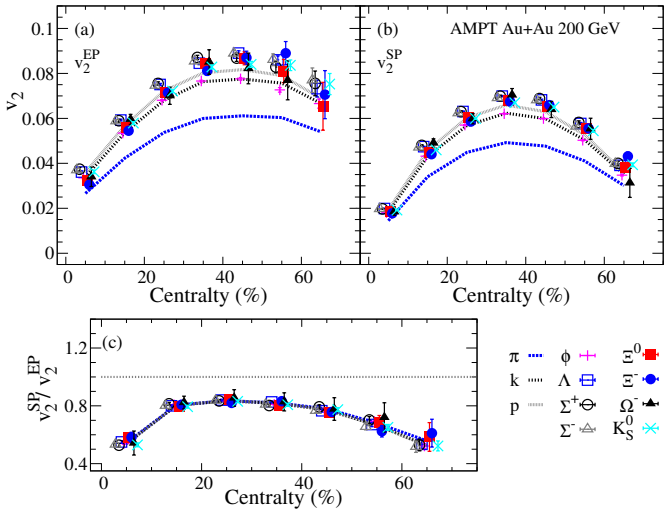

Figure 3. The identified particles centrality dependence of the elliptic flow harmonic with respect to participant and spectator event planes panels (**a**,**b**) respectively. The elliptic flow fluctuations represented by the ratio $v_2^{\mathrm{SP}}/v_2^{\mathrm{EP}}$ are presented in panel (**c**) for Au+Au collisions at $\sqrt{s_{NN}}$ = 200 GeV from the AMPT model.

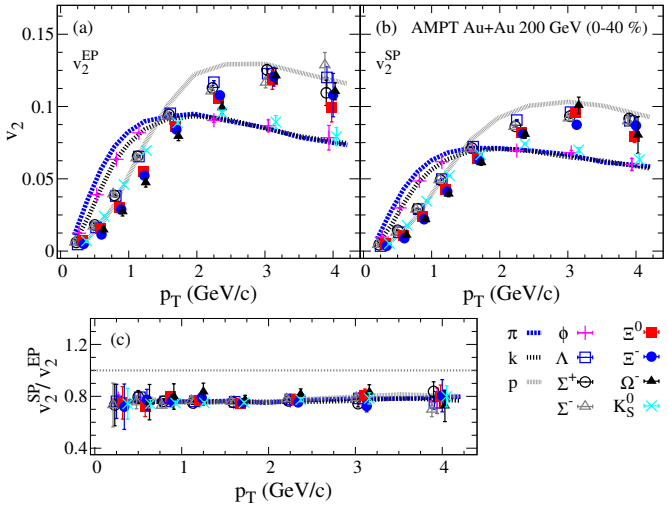

Figure 4. The identified particles p_T dependence of the elliptic flow harmonic with respect to participant and spectator event planes panels (**a**,**b**) respectively. The elliptic flow fluctuations represented by the ratio $v_2^{\mathrm{SP}}/v_2^{\mathrm{EP}}$ are presented in panel (**c**) for Au+Au collisions at $\sqrt{s_{NN}}$ = 200 GeV from the AMPT model.

4. Conclusions

In summary, we studied the centrality and transverse momentum dependence of the identified particles v_2^{SP}, v_2^{EP} and the elliptic flow fluctuations presented by the ratio v_2^{SP}/v_2^{EP} using the AMPT model. The magnitude of the elliptic flow fluctuations is observed to increase from central to mid-central collisions, consistent with the patterns expected from the initial-state eccentricity fluctuations; a weak p_T dependence is also observed. The centrality and p_T dependence of the identified particles v_2^{EP} and v_2^{SP} show the expected mass ordering. However, the elliptic flow fluctuations show no particle species dependence. The integrated and differential elliptic flow fluctuation results indicate the domination of the effect of the initial-state eccentricity fluctuations as expected in the AMPT model. It is suggested that similar investigations of experimental data could display important insight on the ICCING scenario in heavy-ion collisions.

Author Contributions: N.M.; conceptualization, methodology, software, formal analysis, and writing—original draft preparation. X.S., Z.Y., O.E., and R.L.: writing—review, and editing. All authors have read and agreed to the published version of the manuscript.

Funding: This research was funded by the US Department of Energy under contract DE-FG02-94ER40865 (N.M., X.S., Z.Y. and O.E.) and DE-FG02-87ER40331.A008 (R.L.).

Acknowledgments: The authors thank Jacquelyn Noronha-Hostler for the useful discussion and Emily Racow for the language check.

Conflicts of Interest: The authors declare no conflict of interest.

References

1. Heinz, U.W.; Kolb, P.F. Early thermalization at RHIC. *Nucl. Phys.* **2002**, *A702*, 269–280. [CrossRef]
2. Hirano, T.; Heinz, U.W.; Kharzeev, D.; Lacey, R.; Nara, Y. Hadronic dissipative effects on elliptic flow in ultrarelativistic heavy-ion collisions. *Phys. Lett.* **2006**, *B636*, 299–304. [CrossRef]
3. Huovinen, P.; Kolb, P.F.; Heinz, U.W.; Ruuskanen, P.V.; Voloshin, S.A. Radial and elliptic flow at RHIC: Further predictions. *Phys. Lett.* **2001**, *B503*, 58–64. [CrossRef]
4. Hirano, T.; Tsuda, K. Collective flow and two pion correlations from a relativistic hydrodynamic model with early chemical freeze out. *Phys. Rev.* **2002**, *C66*, 054905. [CrossRef]
5. Romatschke, P.; Romatschke, U. Viscosity Information from Relativistic Nuclear Collisions: How Perfect is the Fluid Observed at RHIC? *Phys. Rev. Lett.* **2007**, *99*, 172301. [CrossRef] [PubMed]
6. Luzum, M. Flow fluctuations and long-range correlations: Elliptic flow and beyond. *J. Phys.* **2011**, *G38*, 124026. [CrossRef]
7. Song, H.; Bass, S.A.; Heinz, U.; Hirano, T.; Shen, C. 200 A GeV Au+Au collisions serve a nearly perfect quark-gluon liquid. *Phys. Rev. Lett.* **2011**, *106*, 192301. [CrossRef] [PubMed]
8. Qian, J.; Heinz, U.W.; Liu, J. Mode-coupling effects in anisotropic flow in heavy-ion collisions. *Phys. Rev.* **2016**, *C93*, 064901. [CrossRef]
9. Magdy, N. Beam energy dependence of the anisotropic flow coefficients v_n. *PoS* **2018**, *CPOD2017*, 005.
10. Magdy, N. Viscous Damping of Anisotropic Flow in 7.7–200 GeV Au+Au Collisions. *J. Phys. Conf. Ser.* **2017**, *779*, 012060. [CrossRef]
11. Schenke, B.; Jeon, S.; Gale, C. Anisotropic flow in $\sqrt{s} = 2.76$ TeV Pb+Pb collisions at the LHC. *Phys. Lett.* **2011**, *B702*, 59–63. [CrossRef]
12. Teaney, D.; Yan, L. Non linearities in the harmonic spectrum of heavy ion collisions with ideal and viscous hydrodynamics. *Phys. Rev.* **2012**, *C86*, 044908. [CrossRef]
13. Gardim, F.G.; Grassi, F.; Luzum, M.; Ollitrault, J.Y. Anisotropic flow in event-by-event ideal hydrodynamic simulations of $\sqrt{s_{NN}} = 200$ GeV Au+Au collisions. *Phys. Rev. Lett.* **2012**, *109*, 202302. [CrossRef] [PubMed]
14. Lacey, R.A.; Reynolds, D.; Taranenko, A.; Ajitanand, N.N.; Alexander, J.M.; Liu, F.H.; Gu, Y.; Mwai, A. Acoustic scaling of anisotropic flow in shape-engineered events: Implications for extraction of the specific shear viscosity of the quark gluon plasma. *J. Phys.* **2016**, *G43*, 10LT01. [CrossRef]
15. Voloshin, S.; Zhang, Y. Flow study in relativistic nuclear collisions by Fourier expansion of Azimuthal particle distributions. *Z. Phys. C* **1996**, *70*, 665–672. [CrossRef]
16. Poskanzer, A.M.; Voloshin, S.A. Methods for analyzing anisotropic flow in relativistic nuclear collisions. *Phys. Rev.* **1998**, *C58*, 1671–1678. [CrossRef]
17. Magdy, N. Beam-energy dependence of the azimuthal anisotropic flow from RHIC. *arXiv* **2019**, arXiv:1909.09640.
18. Adam, J.; Adamczyk, L.; Adams, J.R.; Adkins, J.K.; Agakishiev, G.; Aggarwal, M.M.; Ahammed, Z.; Alekseev, I.; Anderson, D.M.; Aoyama, R.; et al. Azimuthal Harmonics in Small and Large Collision Systems at RHIC Top Energies. *Phys. Rev. Lett.* **2019**, *122*, 172301. [CrossRef]
19. Magdy, N. Collision system and beam energy dependence of anisotropic flow fluctuations. *Nucl. Phys.* **2019**, *A982*, 255–258. [CrossRef]
20. Adamczyk, L.; Adams, J.R.; Adkins, J.K.; Agakishiev, G.; Aggarwal, M.M.; Ahammed, Z.; Ajitanand, N.N.; Alekseev, I.; Anderson, D.M.; Aoyama, R.; et al. Azimuthal anisotropy in Cu+Au collisions at $\sqrt{s_{NN}}$ = 200 GeV. *Phys. Rev.* **2018**, *C98*, 014915. [CrossRef]

21. Adamczyk, L.; Adkins, J.K.; Agakishiev, G.; Aggarwal, M.M.; Ahammed, Z.; Ajitanand, N.N.; Alekseev, I.; Anderson, D.M.; Aoyama, R.; Aparin, A.; et al. Harmonic decomposition of three-particle azimuthal correlations at energies available at the BNL Relativistic Heavy Ion Collider. *Phys. Rev.* **2018**, *C98*, 034918. [CrossRef]
22. Alver, B.; Roland, G. Collision geometry fluctuations and triangular flow in heavy-ion collisions. *Phys. Rev.* **2010**, *C81*, 054905. [CrossRef]
23. Chatrchyan, S.; Khachatryan, V.; Sirunyan, A.M.; Tumasyan, A.; Adam, W.; Bergauer, T.; Dragicevic, M.; Eroe, J.; Fabjan, C.; Friedl, M.; et al. Measurement of higher-order harmonic azimuthal anisotropy in PbPb collisions at $\sqrt{s_{NN}}$ = 2.76 TeV. *Phys. Rev.* **2014**, *C89*, 044906. [CrossRef]
24. Alver, B.; Back, B.B.; Baker, M.D.; Ballintijn, M.; Barton, D.S.; Betts, R.R.; Bindel, R.; Busza, W.; Chetluru, V.; Garcia, E.; et al. Importance of correlations and fluctuations on the initial source eccentricity in high-energy nucleus-nucleus collisions. *Phys. Rev.* **2008**, *C77*, 014906. [CrossRef]
25. Alver, B.; Roland, C.; Seals, H.; Wolfs, F.L.H.; Roland, G.; Verdier, R.; Loizides, C.; Holynski, R.; Manly, S.; Li, W.; et al. Non-flow correlations and elliptic flow fluctuations in gold-gold collisions at $\sqrt{s_{NN}}$ = 200 GeV. *Phys. Rev.* **2010**, *C81*, 034915. [CrossRef]
26. Ollitrault, J.Y.; Poskanzer, A.M.; Voloshin, S.A. Effect of flow fluctuations and nonflow on elliptic flow methods. *Phys. Rev.* **2009**, *C80*, 014904. [CrossRef]
27. Adam, J.; Adamczyk, L.; Adams, J.R.; Adkins, J.K.; Agakishiev, G.; Aggarwal, M.M.; Ahammed, Z.; Ajitanand, N.N.; Alekseev, I.; Anderson, D.M.; et al. Correlation Measurements Between Flow Harmonics in Au+Au Collisions at RHIC. *Phys. Lett.* **2018**, *B783*, 459–465. [CrossRef]
28. Qiu, Z.; Heinz, U.W. Event-by-event shape and flow fluctuations of relativistic heavy-ion collision fireballs. *Phys. Rev.* **2011**, *C84*, 024911. [CrossRef]
29. Adare, A.; Afanasiev, S.; Aidala, C.; Ajitanand, N.N.; Akiba, Y.; Al-Bataineh, H.; Alexander, J.; Aoki, K.; Aramaki, Y.; Atomssa, E.T.; et al. Measurements of Higher-Order Flow Harmonics in Au+Au Collisions at $\sqrt{s_{NN}}$ = 200 GeV. *Phys. Rev. Lett.* **2011**, *107*, 252301. [CrossRef]
30. Aad, G.; Abbott, B.; Abdallah, J.; Khalek, S.A.; Aben, R.; Abi, B.; Abolins, M.; AbouZeid, O.S.; Abramowicz, H.; Abreu, H.; et al. Measurement of event-plane correlations in $\sqrt{s_{NN}}$ = 2.76 TeV lead-lead collisions with the ATLAS detector. *Phys. Rev.* **2014**, *C90*, 024905. [CrossRef]
31. Aad, G.; Abajyan, T.; Abbott, B.; Abdallah, J.; Khalek, S.A.; Abdelalim, A.A.; Aben, R.; Abi, B.; Abolins, M.; AbouZeid, O.S.; et al. Measurement of the correlation between flow harmonics of different order in lead-lead collisions at $\sqrt{s_{NN}}$=2.76 TeV with the ATLAS detector. *Phys. Rev.* **2015**, *C92*, 034903. [CrossRef]
32. Niemi, H.; Denicol, G.S.; Holopainen, H.; Huovinen, P. Event-by-event distributions of azimuthal asymmetries in ultrarelativistic heavy-ion collisions. *Phys. Rev.* **2013**, *C87*, 054901. [CrossRef]
33. Gardim, F.G.; Noronha-Hostler, J.; Luzum, M.; Grassi, F. Effects of viscosity on the mapping of initial to final state in heavy ion collisions. *Phys. Rev.* **2015**, *C91*, 034902. [CrossRef]
34. Fu, J. Centrality dependence of mapping the hydrodynamic response to the initial geometry in heavy-ion collisions. *Phys. Rev.* **2015**, *C92*, 024904. [CrossRef]
35. Holopainen, H.; Niemi, H.; Eskola, K.J. Event-by-event hydrodynamics and elliptic flow from fluctuating initial state. *Phys. Rev.* **2011**, *C83*, 034901. [CrossRef]
36. Qin, G.Y.; Petersen, H.; Bass, S.A.; Muller, B. Translation of collision geometry fluctuations into momentum anisotropies in relativistic heavy-ion collisions. *Phys. Rev.* **2010**, *C82*, 064903. [CrossRef]
37. Gale, C.; Jeon, S.; Schenke, B.; Tribedy, P.; Venugopalan, R. Event-by-event anisotropic flow in heavy-ion collisions from combined Yang-Mills and viscous fluid dynamics. *Phys. Rev. Lett.* **2013**, *110*, 012302. [CrossRef]
38. Liu, P.; Lacey, R.A. Acoustic scaling of linear and mode-coupled anisotropic flow; implications for precision extraction of the specific shear viscosity. *arXiv* **2018**, arXiv:1802.06595.
39. Borghini, N.; Dinh, P.M.; Ollitrault, J.Y. A New method for measuring azimuthal distributions in nucleus-nucleus collisions. *Phys. Rev.* **2001**, *C63*, 054906. [CrossRef]
40. Miller, M.; Snellings, R. Eccentricity fluctuations and its possible effect on elliptic flow measurements. *arXiv* **2003**, arXiv:0312008.
41. Manly, S.; Phobos, C. System size, energy and pseudorapidity dependence of directed and elliptic flow at RHIC. *Nucl. Phys.* **2006**, *A774*, 523–526. [CrossRef]

42. Voloshin, S.A. Toward the energy and the system size dependece of elliptic flow: Working on flow fluctuations. In Proceedings of the 22nd Winter Workshop on Nuclear Dynamics (WWND 2006), La Jolla, CA, USA, 11–19 March 2006.
43. Gardim, F.G.; Grassi, F.; Hama, Y.; Luzum, M.; Ollitrault, J.Y. Directed flow at mid-rapidity in event-by-event hydrodynamics. *Phys. Rev.* **2011**, *C83*, 064901. [CrossRef]
44. Schenke, B.; Shen, C.; Tribedy, P. Hybrid Color Glass Condensate and hydrodynamic description of the Relativistic Heavy Ion Collider small system scan. *Phys. Lett. B* **2020**, *803*, 135322. [CrossRef]
45. Werner, K. Strings, pomerons, and the venus model of hadronic interactions at ultrarelativistic energies. *Phys. Rep.* **1993**, *232*, 87–299. [CrossRef]
46. Shen, C.; Schenke, B. Dynamical initial state model for relativistic heavy-ion collisions. *Phys. Rev. C* **2018**, *97*, 024907. [CrossRef]
47. Akamatsu, Y.; Asakawa, M.; Hirano, T.; Kitazawa, M.; Morita, K.; Murase, K.; Nara, Y.; Nonaka, C.; Ohnishi, A. Dynamically integrated transport approach for heavy-ion collisions at high baryon density. *Phys. Rev. C* **2018**, *98*, 024909. [CrossRef]
48. Mohs, J.; Ryu, S.; Elfner, H. Particle Production via Strings and Baryon Stopping within a Hadronic Transport Approach. *J. Phys. G* **2020**, *47*, 065101. [CrossRef]
49. Steinheimer, J.; Mitrovski, M.; Schuster, T.; Petersen, H.; Bleicher, M.; Stoecker, H. Strangeness fluctuations and MEMO production at FAIR. *Phys. Lett. B* **2009**, *676*, 126–131. [CrossRef]
50. Martinez, M.; Sievert, M.D.; Wertepny, D.E.; Noronha-Hostler, J. Initial state fluctuations of QCD conserved charges in heavy-ion collisions. *arXiv* **2019**, arXiv:1911.10272.
51. Giacalone, G.; Noronha-Hostler, J.; Ollitrault, J.Y. Relative flow fluctuations as a probe of initial state fluctuations. *Phys. Rev. C* **2017**, *95*, 054910. [CrossRef]
52. Alba, P.; Mantovani Sarti, V.; Noronha, J.; Noronha-Hostler, J.; Parotto, P.; Vazquez, I.P.; Ratti, C. Effect of the QCD equation of state and strange hadronic resonances on multiparticle correlations in heavy ion collisions. *arXiv* **2017**, arXiv:1711.05207.
53. Adamczyk, L.; Adkins, J.K.; Agakishiev, G.; Aggarwal, M.M.; Ahammed, Z.; Alekseev, I.; Aparin, A.; Arkhipkin, D.; Aschenauer, E.C.; Averichev, G.S.; et al. Centrality and transverse momentum dependence of elliptic flow of multistrange hadrons and ϕ meson in Au+Au collisions at $\sqrt{s_{NN}}$ = 200 GeV. *Phys. Rev. Lett.* **2016**, *116*, 062301. [CrossRef] [PubMed]
54. Adler, C.; Strobele, H.; Denisov, A.; Garcia, E.; Murray, M.; White, S. The RHIC zero-degree calorimeters. *Nucl. Instrum. Methods* **2001**, *A461*, 337–340. [CrossRef]
55. Adams, J.; Ewigleben, A.; Garrett, S.; He, W.; Huang, T.; Jacobs, P.M.; Ju, X.; Lisa, M.A.; Lomnitz, M.; Pak, R.; et al. The STAR Event Plane Detector. *arXiv* **2019**, arXiv:1912.05243.
56. Lin, Z.W.; Ko, C.M.; Li, B.A.; Zhang, B.; Pal, S. A Multi-phase transport model for relativistic heavy ion collisions. *Phys. Rev.* **2005**, *C72*, 064901.[CrossRef]
57. Ma, G.L.; Lin, Z.W. Predictions for $\sqrt{s_{NN}} = 5.02$ TeV Pb+Pb Collisions from a Multi-Phase Transport Model. *Phys. Rev.* **2016**, *C93*, 054911. [CrossRef]
58. Ma, G.L. Decomposition of the jet fragmentation function in high-energy heavy-ion collisions. *Phys. Rev.* **2013**, *C88*, 021902. [CrossRef]
59. Ma, G.L. Medium modifications of jet shapes in Pb+Pb collisions at $\sqrt{s_{NN}}$ = 2.76 TeV within a multiphase transport model. *Phys. Rev.* **2014**, *C89*, 024902. [CrossRef]
60. Bzdak, A.; Ma, G.L. Elliptic and triangular flow in p+Pb and peripheral Pb+Pb collisions from parton scatterings. *Phys. Rev. Lett.* **2014**, *113*, 252301. [CrossRef]
61. Nie, M.W.; Huo, P.; Jia, J.; Ma, G.L. Multiparticle azimuthal cumulants in p+Pb collisions from a multiphase transport model. *Phys. Rev.* **2018**, *C98*, 034903. [CrossRef]
62. Magdy, N.; Nie, M.W.; Huang, L.; Ma, G.L.; Lacey, R. An extended $R^{(2)}_{\Psi_m}(\Delta S_2)$ correlator for detecting and characterizing the Chiral Magnetic Wave. *arXiv* **2020**, arXiv:2003.02396.
63. Wang, X.N.; Gyulassy, M. HIJING: A Monte Carlo model for multiple jet production in p p, p A and A A collisions. *Phys. Rev.* **1991**, *D44*, 3501–3516. [CrossRef]
64. Zhang, B. ZPC 1.0.1: A Parton cascade for ultrarelativistic heavy ion collisions. *Comput. Phys. Commun.* **1998**, *109*, 193–206. [CrossRef]
65. Li, B.A.; Ko, C.M. Formation of superdense hadronic matter in high-energy heavy ion collisions. *Phys. Rev.* **1995**, *C52*, 2037–2063. [CrossRef] [PubMed]

66. Bilandzic, A.; Snellings, R.; Voloshin, S. Flow analysis with cumulants: Direct calculations. *Phys. Rev.* **2011**, *C83*, 044913. [CrossRef]
67. Bilandzic, A.; Christensen, C.H.; Gulbrandsen, K.; Hansen, A.; Zhou, Y. Generic framework for anisotropic flow analyses with multiparticle azimuthal correlations. *Phys. Rev.* **2014**, *C89*, 064904. [CrossRef]
68. Jia, J.; Zhou, M.; Trzupek, A. Revealing long-range multiparticle collectivity in small collision systems via subevent cumulants. *Phys. Rev.* **2017**, *C96*, 034906. [CrossRef]
69. Gajdošová, K. Investigations of anisotropic collectivity using multi-particle correlations in pp, p–Pb and Pb–Pb collisions. *Nucl. Phys.* **2017**, *A967*, 437–440. [CrossRef]
70. Snellings, R. Elliptic Flow: A Brief Review. *New J. Phys.* **2011**, *13*, 055008. [CrossRef]
71. Voloshin, S.A.; Poskanzer, A.M.; Tang, A.; Wang, G. Elliptic flow in the Gaussian model of eccentricity fluctuations. *Phys. Lett.* **2008**, *B659*, 537–541. [CrossRef]
72. Wang, G. Anisotropic flow in Au Au and Cu Cu at 62-GeV and 200-GeV. *Nucl. Phys. A* **2006**, *774*, 515–518. [CrossRef]
73. Ma, L.; Ma, G.; Ma, Y. Anisotropic flow and flow fluctuations for Au + Au at $\sqrt{s_{NN}}$ = 200 GeV in a multiphase transport model. *Phys. Rev. C* **2014**, *89*, 044907. [CrossRef]
74. Ma, G.L.; Bzdak, A. Long-range azimuthal correlations in proton–proton and proton–nucleus collisions from the incoherent scattering of partons. *Phys. Lett. B* **2014**, *739*, 209–213. [CrossRef]
75. Singha, S.; Nasim, M. Scaling of elliptic flow in heavy-ion collisions with the number of constituent quarks in a transport model. *Phys. Rev. C* **2016**, *93*, 034908. [CrossRef]
76. Nayak, K.; Singha, S.; Nasim, M.; Mohanty, B. Study of re-scattering effect on elliptic flow and production of resonances using AMPT. *DAE Symp. Nucl. Phys.* **2017**, *62*, 962–963.
77. Magdy, N. *Collision System Dependence of Anisotropic Flow, Flow Fluctuations and Mixed Harmonic Correlations at STAR Energies*; Quark Matter; Stony Brook University: Stony Brook, NY, USA, 2018.